THE JOURNAL OF BIOLOGICAL CHEMISTRY VOL. 284, NO. 38, pp. 25704–25713, September 18, 2009

The Development of a Metabolic Disease Phenotype in CTP: Phosphoethanolamine Cytidylyltransferase-deficient Mice*[S]

Received for publication, May 21, 2009, and in revised form, July 20, 2009 Published, JBC Papers in Press, July 22, 2009, DOI 10.1074/jbc.M109.023846

Morgan D. Fullerton, Fatima Hakimuddin, Arend Bonen, and Marica Bakovic[1]

From the Department of Human Health and Nutritional Sciences, University of Guelph, Guelph, Ontario N1G 2W1, Canada

Phosphatidylethanolamine (PE) is an important inner membrane phospholipid mostly synthesized *de novo* via the PE-Kennedy pathway and by the decarboxylation of phosphatidylserine. CTP:phosphoethanolamine cytidylyltransferase (*Pcyt2*) catalyzes the formation of CDP-ethanolamine, which is often the rate regulatory step in the PE-Kennedy pathway. In the current investigation, we show that the reduced CDP-ethanolamine formation in $Pcyt2^{+/-}$ mice limits the rate of PE synthesis and increases the availability of diacylglycerol. This results in the increased formation of triglycerides, which is facilitated by stimulated *de novo* fatty acid synthesis and increased uptake of pre-existing fatty acids. $Pcyt2^{+/-}$ mice progressively accumulate more diacylglycerol and triglycerides with age and have modified fatty acid composition, predominantly in PE and triglycerides. $Pcyt2^{+/-}$ additionally have an inherent blockage in fatty acid utilization as energy substrate and develop impaired tolerance to glucose and insulin at an older age. Accordingly, gene expression analyses demonstrated the up-regulation of the main lipogenic genes and down-regulation of mitochondrial fatty acid β-oxidation genes. These data demonstrate for the first time that to preserve membrane PE phospholipids, *Pcyt2* deficiency generates compensatory changes in triglyceride and energy substrate metabolism, resulting in a progressive development of liver steatosis, hypertriglyceridemia, obesity, and insulin resistance, the main features of the metabolic syndrome.

Phosphatidylethanolamine (PE)[2] is the major inner leaflet phospholipid in cellular membranes, and it plays important roles in membrane integrity, cell division, cytokinesis, autophagy, and blood coagulation (1). Phospholipases degrade PE to the secondary substrates diacylglycerols (DAG), phosphatidic acid, and free fatty acids (FA), which are involved in energy metabolism and various cell-signaling cascades. *N*-Acylated PE is a main source of endogenous cannabinoids including *N*-arachidonyl-ethanolamine anandamide (2), and PE is a donor of the phosphoethanolamine moiety of glycosylphosphatidylinositol anchors, ensuring the linking of the carboxyl terminus of various proteins to the plasma membrane (3). PE also serves as a natural ligand for steroidogenic factor-1 (4) and liver receptor homologue 1 (5), transcription factors involved in the regulation of gene function. In *Drosophila*, PE completely substitutes for cholesterol in the feedback regulation of SREBPs (sterol regulatory element-binding proteins) (6), which highlights its importance in the nuclear control of lipid metabolism.

The CDP-ethanolamine (PE-Kennedy) pathway (Fig. 1) is responsible for the *de novo* synthesis of PE and is essential for the production of PE plasmalogens (7, 8), whereas the decarboxylation of phosphatidylserine (PS) produces a significant portion of mitochondrial PE (9) and in some cell cultures can become a dominant pathway for PE synthesis (10). PE may also be formed from pre-existing phospholipids by base exchange mechanisms; however, this is a quantitatively minor pathway (11). In the PE-Kennedy pathway, ethanolamine is first phosphorylated by ethanolamine kinase to phosphoethanolamine, which is converted to CDP-ethanolamine by CTP:phosphoethanolamine cytidylyltransferase (ET). In the final step of the pathway, CDP-ethanolamine:1,2-diacylglycerol ethanolaminephosphotransferase catalyzes the formation of PE from CDP-ethanolamine and DAG. CDP-ethanolamine:1,2-diacylglycerol ethanolaminephosphotransferase alternatively couples CDP-ethanolamine with alkylacylglycerols, derived in peroxisomes, to produce alkylacyl (plasmanyl) PE, which is further modified in the mitochondria to the final vinyl-ether (plasmalogen) PE. Multiple isoforms of kinases and phosphotransferases have been identified that share substrates for both the choline and ethanolamine branches of the Kennedy pathway; yet ET is produced by a single gene (*Pcyt2*) and is specific for the ethanolamine branch of the pathway (1).

The *Pcyt2* gene has been cloned and characterized for yeast, human, rat, and mouse (12–15). It gives rise to two evolutionarily conserved splice variants, with distinct tissue expression and catalytic properties (16). Murine and human *Pcyt2* promoters have been isolated and initially characterized (15, 17). The human promoter can be regulated by early growth response factor 1 and nuclear factor κB, and a lower *de novo* synthesis and PE content in human breast cancer cells was attributed to decreased *Pcyt2* gene regulation by early growth response factor 1 (18). The regulation and function of the *Pcyt2* gene has been recently reviewed (1).

Although it is not firmly established how the supply of alkylacylglycerols regulates the production of plasmalogens, DAG availability can control the flux through the PE-Kennedy pathway under certain conditions (19, 20). The possibility that sub-

* This work was supported by an Ontario Graduate Scholarship (to M. D. F.) and Operating Grants MOP-68962 and 410-2007-86448 from the Canadian Institutes of Health Research (to M. B.).

[S] The on-line version of this article (available at http://www.jbc.org) contains supplemental Fig. S1 and supplemental Table S1.

[1] To whom correspondence should be addressed: Animal Science and Nutrition Bldg., Rm. 346, University of Guelph, Guelph, Ontario N1G 2W1, Canada. Tel.: 519-824-4120, Ext. 53764; Fax: 519-763-5902; E-mail: mbakovic@uoguelph.ca.

[2] The abbreviations used are: PE, phosphatidylethanolamine; DAG, diacylglycerol; FA, fatty acid; PS, phosphatidylserine; TG, triglyceride; PBS, phosphate-buffered saline; PC, phosphatidylcholine; DGAT, diacylglycerol acyltransferase; IPGTT, intraperitoneal glucose tolerance test.

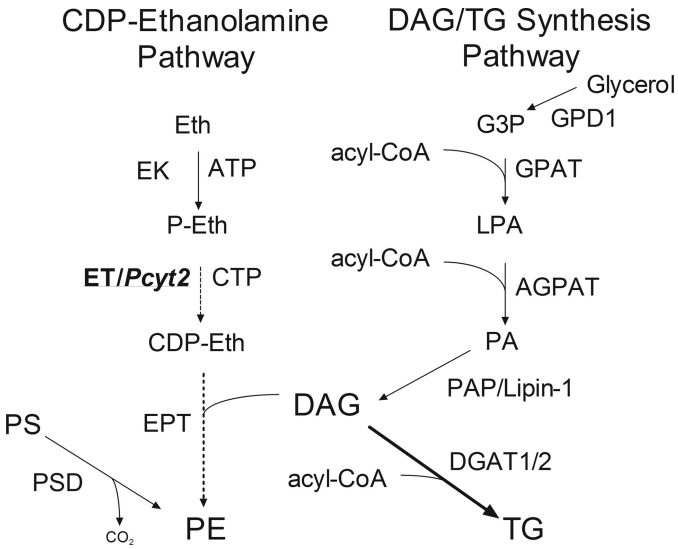

FIGURE 1. **CDP-ethanolamine, DAG, and TG synthetic pathways.** *Eth*, ethanolamine; *EK*, ethanolamine kinase; *P-Eth*, phosphoethanolamine; *ET/Pcyt2*, CTP:phosphoethanolamine cytidylyltransferase; *CDP-Eth*, CDP-ethanolamine; *EPT*, CDP-ethanolamine 1,2-diacylglycerol ethanolaminephosphotransferase; *PE*, phosphatidylethanolamine; *GPD1*, glycerol-3-phosphate dehydrogenase 1; *G3P*, glycerol-3-phosphate; *GPAT*, glycerol 3-phosphate acyltransferase; *LPA*, lysophosphatidic acid; *AGPAT*, 1-acylglycerol-3-phosphate acyltransferase; *PA*, phosphatidic acid; *PAP/Lipin-1*, phosphatidic acid phosphatase; *DAG*, diacylglycerol; *DGAT1/2*, diacylglycerol acyltransferase 1/2; *PSD*, PS decarboxylase.

strate supply controls the Kennedy pathway has also been shown for ethanolamine (7, 21). Thus it is very likely that the PE synthesis via this pathway is coordinately regulated by the availability of both substrates, CDP-ethanolamine (via *Pcyt2*) and DAG, which is very relevant for the current investigation.

We have previously described the deletion of *Pcyt2* in mice, where null embryos are lethal prior to embryonic day 8.5 and heterozygous ($Pcyt2^{+/-}$) mice maintain normal PE levels despite reduced formation of CDP-ethanolamine and reduced flux through the *de novo* pathway (22). This demonstrated that *Pcyt2* is essential during murine development and that PE content cannot be compensated by the mitochondrial decarboxylation of PS. In the current investigation, we establish that reduced formation of CDP-ethanolamine in $Pcyt2^{+/-}$ mice limits the rate of PE synthesis. This increases the availability of DAG and causes a shift in triglyceride (TG) and energy substrate metabolism leading to development of adult stage obesity, liver steatosis, hypertriglyceridemia, and a resistance to the effects of insulin.

EXPERIMENTAL PROCEDURES

Animals—$Pcyt2^{+/-}$ mice were generated as described previously (22). All of the procedures conducted were approved by the University of Guelph Animal Care Committee and were in accordance with guidelines of the Canadian Council on Animal Care. The mice were exposed to a 12-h light/dark cycle beginning with light at 7:00 a.m. Male and female mice were fed *ad libitum* a standardized diet (Harlan Teklad S-2335) and had free access to water. Aside from weight gain analyses, male mice were used for all experiments.

Determination of Tissue and Plasma Lipid Content—Total lipids from plasma, liver, and muscle were extracted by the method of Bligh and Dyer (23). The lipids were extracted by chloroform:methanol (1:2) by vortexing for 30 s. Chloroform and water were subsequently added to obtain a final volume ratio of chloroform:methanol:water (1:1:0.9). The lipid-containing chloroform phase was dried under a stream of nitrogen, resuspended in a constant volume of chloroform or isopropanol, and spotted onto silica gel 60 plates. Phospholipids (PE, PS, and phosphatidylcholine-PC) were separated using a solvent system of chloroform/methanol/acetic acid/water (25:15:4:2, v/v/v/v) and neutral lipids (TG and DAG) by using heptane/isopropyl ether/acetic acid (60:40:3, v/v/v). Authentic lipid standards were run in parallel to the samples, and the plates were sprayed with aniline naphthalene sulfonic acid and exposed to UV light for visualization and quantification by densitometry as previously described (24).

The amount of PE was additionally determined in primary hepatocytes (18). Briefly, the cells were radiolabeled with 0.5 μCi of [^{14}C]ethanolamine (55 Ci/mmol; ARC Inc.) per 6-well dish for 24 h, and [^{14}C]PE was isolated as described above and determined by liquid scintillation counting. In addition, tissue TG and cholesterol as well as plasma glucose, free FAs, TG, and cholesterol were determined using standard kits (Wako Chemicals). Collected plasma was from mice fasted 12–16 h before analyses.

Determination of Fatty Acid Composition—Liver and plasma phospholipids (PE, PC, and PS) and neutral lipids (DAG and TG) were separated by TLC as described above, then hydrolyzed, and transmethylated with 6% H_2SO_4 in methanol at 80 °C for 3 h. The reactions were cooled down to room temperature, and methylated FAs were extracted by phase separation by the addition of 3 ml of petroleum ether and centrifugation at 1,000 × *g* for 15 min at 4 °C. Methylated FA species from individual lipids were determined by gas-liquid chromatography (HP 5890 Series II; Hewlett Packard) as described (25).

Liver Histology and Isolation of Primary Hepatocytes—To examine liver histology, fresh livers from three or four animals were dissected and fixed in 10% formalin in phosphate-buffered saline (PBS) and embedded in paraffin. 10-μm sections were stained with hematoxylin and eosin and visualized by light microscopy. Primary hepatocytes were isolated as described (26, 27) with slight modification. The livers were perfused with an EGTA buffer (140 mM NaCl, 6.7 mM KCl, 10 mM HEPES, and 50 μM EGTA, pH 7.4) at 8 ml/min and then with a solution (67 mM NaCl, 6.7 mM KCl, 5 mM $CaCl_2 \cdot 2H_2O$, and 100 mM HEPES, pH 7.6) containing 0.5% collagenase at 6 ml/min through the inferior vena cava after clamping of the superior vena cava and cutting of the portal vein. Cell viability was assessed using trypan blue exclusion and typically was greater than 95%. The cells (1×10^5 cells/60-mm dish) were platted on 6-well plates (Primari^{TM}; BD) and allowed to attach for 2 h in Williams' medium E (Invitrogen). Unattached cells were removed and replaced with the complete Williams' medium E containing 10% fetal bovine serum (Sigma) and 1% antibiotic-antimytotic solution (Invitrogen). Isolated hepatocytes were incubated overnight at 37 °C, and the experiments were performed the following day.

Hepatic FA Uptake and Transporters—Primary hepatocytes (~0.5×10^6 cells) were radiolabeled with bovine serum albu-

min-complexed [^{3}H]oleate (0.5 μCi/well, 22.7 Ci/mmol; PerkinElmer Life Sciences) for 1, 3, 5, and 8 min. The radiolabeled hepatocytes were washed and lysed in a homogenization buffer (10 mM Tris-HCl, pH 7.4, 1 mM EDTA, 10 mM NaF), and the cell-associated radioactivity was determined by liquid scintillation counting. For FA transporter expression, liver and muscle, plasma membrane-fatty acid-binding protein (FABPpm), fatty acid translocase (FAT/CD36), and fatty acid transport proteins 1 and 4 (FATP1 and FATP4) were characterized by immunoblotting as previously described (28). Ponceau S was utilized as a loading control.

Hepatic Glycerol Uptake and Glycerolipid Metabolism—For pulse experiments, primary hepatocytes were labeled with 1 μCi of [^{3}H]glycerol (20 Ci/mmol; ARC Inc.) in the presence of 50 μM unlabeled glycerol or with 0.5 μCi of [^{3}H]oleate for 1, 2, and 4 h. [^{3}H]glycerol was added directly to the cells, whereas [^{3}H]oleate was first preincubated with bovine serum albumin-complexed sodium oleate (molar ratio was 4:1). For pulse-chase experiments, hepatocytes were pulsed for 2 h with 0.1 μCi of [^{14}C]ethanolamine in the presence of 50 μM unlabeled ethanolamine or 2.5 μCi of [^{3}H]glycerol in the presence of 50 μM unlabeled glycerol in complete medium. Radiolabeled medium was then removed, and the cells were washed with PBS and chased with a medium containing an excess (250 μM) of unlabeled ethanolamine or glycerol for 1, 2, and 4 h. For analyses, the cells were washed twice with ice-cold PBS and collected in PBS. Radiolabeled total phospholipids, PE, DAG, and TG were isolated by TLC as described for the plasma and tissues above and determined by liquid scintillation counting.

Glycerol uptake was assayed as previously described (29), with some modifications. Isolated hepatocytes were incubated in PBS supplemented with 6 mM glucose and 1 μCi of [^{3}H]glycerol for 1, 2, and 3 min to ensure linearity in glycerol uptake. After each incubation time, the cells were washed with ice-cold PBS containing increasing concentrations of unlabeled glycerol (10, 50, and 100 mM) and lysed with 10% SDS. The glycerol uptake in nmol/mg/min was determined from the cell-associated radioactivity as described above for the [^{3}H]glycerol pulse and pulse-chase experiments.

Hepatic FA Oxidation—Primary hepatocytes ($\sim$1.2 $\times$ 10^6 cells) were cultured 24 h in 60-mm dishes as described above and then radiolabeled with 1 μCi/dish [^{14}C]oleate (55 mCi/mmol) for 1.5 h in an assay mixture of 1 mM carnitine, 250 μM "cold" sodium oleate complexed to 2.5% FA-free bovine serum albumin and complete William's medium E (29). After addition of the radiolabeled mixture (3 ml), the dish containing the cells was placed uncovered into an empty 100-mm dish with two rubber stoppers fitted on the lid. A small cup was also placed in a holder inside the larger dish, and the system was made air tight with parafilm and incubated for 2 h at 37 °C. After the incubation, 200 μl of 1 M benzethonium hydroxide was added by syringe into the small cup through the rubber stopper. Three ml of 3 M H_2SO_4 was added through another rubber stopper directly to the cells to liberate both [^{14}C]CO_2 and the labeled trichloroacetic acid cycle intermediates. The released [^{14}C]CO_2 was trapped with benzethonium hydroxide for 2 h, and the radioactivity was determined by liquid scintillation counting. Duplicate plates were utilized for protein determination using the BCA protein kit (Pierce).

In Vivo Lipid Radiolabeling—The mice were fasted for 4 h prior to an intraperitoneal injection of 5 μCi of [^{3}H]acetate (20 Ci/mmol) diluted in 0.9% saline in the presence of 250 μM unlabeled sodium acetate. The mice were sacrificed after 1 h, and 100–200-mg portions of liver were immediately homogenized in two volumes of PBS. Total lipids were extracted by the method of Bligh and Dyer as described above and then saponified in ethanolic 0.5 M NaOH for 3 h at 70 °C. Nonsaponified lipids (mainly free cholesterol) were extracted three times with petroleum ether, and radioactivity was determined by liquid scintillation counting. Remaining saponified lipids (phospholipids, neutral lipids, and cholesterol ester) were acidified with 6 N HCl, extracted three times with petroleum ether, and evaporated to dryness. The incorporation of [^{3}H]acetate into total phospholipids, PE, sphingomyelin, DAG, TG, free FAs, free cholesterol, and cholesterol esters was determined by TLC as described above.

Food Intake and Energy Expenditure—Mice from each genotype were housed individually for 5 days, after which the consumption of their diet was weighed at 8:00 a.m. for 10 consecutive days. For energy expenditure, the mice were weighed prior to the removal of all food. After 24 h and *ad libitum* access to water, the mice were weighed, and an estimation of energy expenditure was made from the change in body weight. Indirect calorimetry (Oxymax; Columbus Instruments) was performed over a 24-h period from which the respiratory quotient: VCO_2/VO_2) was determined.

Glucose Tolerance Test—The mice were fasted 6 h, and after a base-line saphenous vein blood sample, 2 mg/kg glucose (in 0.9% saline) was administered via intraperitoneal injection. Blood sample for glucose and insulin determination were taken for up to 2 h, where blood glucose was determined by a monitoring system (Ascensia Elite XL). Insulin was determined using an enzyme-linked immunosorbent assay kit (Linco).

RNA Isolation and Expression Analyses—Tissue harvesting, RNA extraction, and first strand cDNA synthesis was performed as described previously (22). The main lipogenic genes and mitochondrial fatty acid β-oxidation genes were analyzed in the linear phase of PCR, using the optimal reaction cycle conditions. Liver and skeletal muscle mRNA was expressed relative to β-actin. The gene lists, primers, and cycle conditions are available upon request.

Statistical Analyses—All of the data are expressed as the means $\pm$ S.E. Statistical significance (for *Pcyt2*$^{+/-}$ relative to wild-type littermate controls) were determined using two-tailed, unpaired Student's *t* test or linear regression. Growth curve and metabolic chamber data were analyzed by one-way analysis of variance. GraphPad Prism 4 software was used for all of the statistical calculations. For all radiolabeling experiments, the specific activity was adjusted to account for the amount of unlabeled substrate.

RESULTS

Pcyt2$^{+/-}$ *Mice Have Reduced PE Synthesis and Degradation*—In our previous study (22) we performed specific radiolabeling of the PE-Kennedy pathway using [^{14}C]ethanolamine and

established that the rate of formation of CDP-ethanolamine was significantly reduced and was therefore limiting PE synthesis in *Pcyt2*$^{+/-}$ mice. We also established that despite the reduced rate of PE synthesis, the tissue PE content remained unmodified (as was the total PS and PC content) (22). In the current investigation, PE homeostasis was examined in isolated primary hepatocytes from 40-week-old *Pcyt2*$^{+/-}$ mice and littermate controls. When the hepatocytes were compared for total PE content, no differences were observed between genotypes. On the other hand, the rate of PE synthesis from [^{3}H]glycerol was significantly lower in the *Pcyt2*$^{+/-}$ hepatocytes compared with littermate controls (0.01 ± 0.003 *versus* 0.024 ± 0.0051 nmol/mg/h) (Fig. 2*A*), as was observed initially with [^{14}C]ethanolamine (22).

Because total PE content was unaffected by the reduced rate of PE synthesis, we also determined the rate of PE degradation by pulse-chase experiments, using [^{14}C]ethanolamine as a measure of the PE-Kennedy pathway and [^{3}H]glycerol as a measure of all PE synthetic pathways. Both types of labeling revealed similarly reduced PE degradation in *Pcyt2*$^{+/-}$ hepatocytes relative to controls. With [^{3}H]glycerol pulse-chase experiments, the degradation rates were 0.019 ± 0.008 *versus* 0.04 ± 0.07 nmol/mg/h, and with those with [^{14}C]ethanolamine were 0.11 ± 0.06 *versus* 0.37 ± 0.05 nmol/mg/h (Fig. 2, *B* and *C*). Taken together, these data demonstrate that reduced PE catabolism in heterozygous hepatocytes represents a homeostatic response to reduced PE synthesis via the Kennedy pathway. This type of adaptation allows *Pcyt2*$^{+/-}$ animals to maintain constant membrane PE content, because mitochondrial PS decarboxylation is not affected (22). Similar homeostatic effects were observed in animal models for other membrane phospholipids, such as for PS in PS synthase 2-deficient mice (30) or for PC in a choline kinase α-deficient mice (31) where reduced PS and PC degradations were mechanisms to preserve their membrane content.

Pcyt2$^{+/-}$ *Mice Develop Adult Onset Obesity and Fatty Liver*—*Pcyt2*$^{+/-}$ mice were not phenotypically different from littermate controls during early adulthood (22). However, when monitored for a longer period, both male and female *Pcyt2*$^{+/-}$ mice progressively gain more weight than the same sex littermate controls (Fig. 3*A*). At younger ages mice did not differ in adipose and liver tissue mass and lipid deposition, but weight differences became robust in older *Pcyt2*$^{+/-}$ mice (Fig. 3*A*, *inset*). *Pcyt2*$^{+/-}$ epididymal, subcutaneous, and renal adipose mass increased 24.5, 13, and 23%, respectively, and liver mass was 28% higher than in controls (Fig. 3*B*). In addition, liver DAG content was elevated (1.8 ± 0.1 *versus* 1.3 ± 0.1 mg/or ~60%), and liver TG content was almost 2-fold higher in *Pcyt2*$^{+/-}$ mice (Fig. 4*A*). Histological analyses of *Pcyt2*$^{+/-}$ liver (Fig. 4*B*) revealed large vacuole-like formations corresponding to lipid droplets, in which TG had accumulated, demonstrating that *Pcyt2*$^{+/-}$ mice develop not only adult onset obesity but also liver steatosis.

Pcyt2$^{+/-}$ *Mice Develop Hypertriglyceridemia*—In addition to progressive weight gain and increased hepatic lipid accumulation, older *Pcyt2*$^{+/-}$ mice also had altered plasma lipid profiles compared with littermate controls. Total plasma TG was 55.6% higher in *Pcyt2*$^{+/-}$ animals and predominantly associated with very low density lipoprotein fractions (Figs. 3*D* and 4*C*). Total plasma PC and cholesterol contents were unchanged between genotypes, and their distribution among various lipoprotein fractions also was not affected.

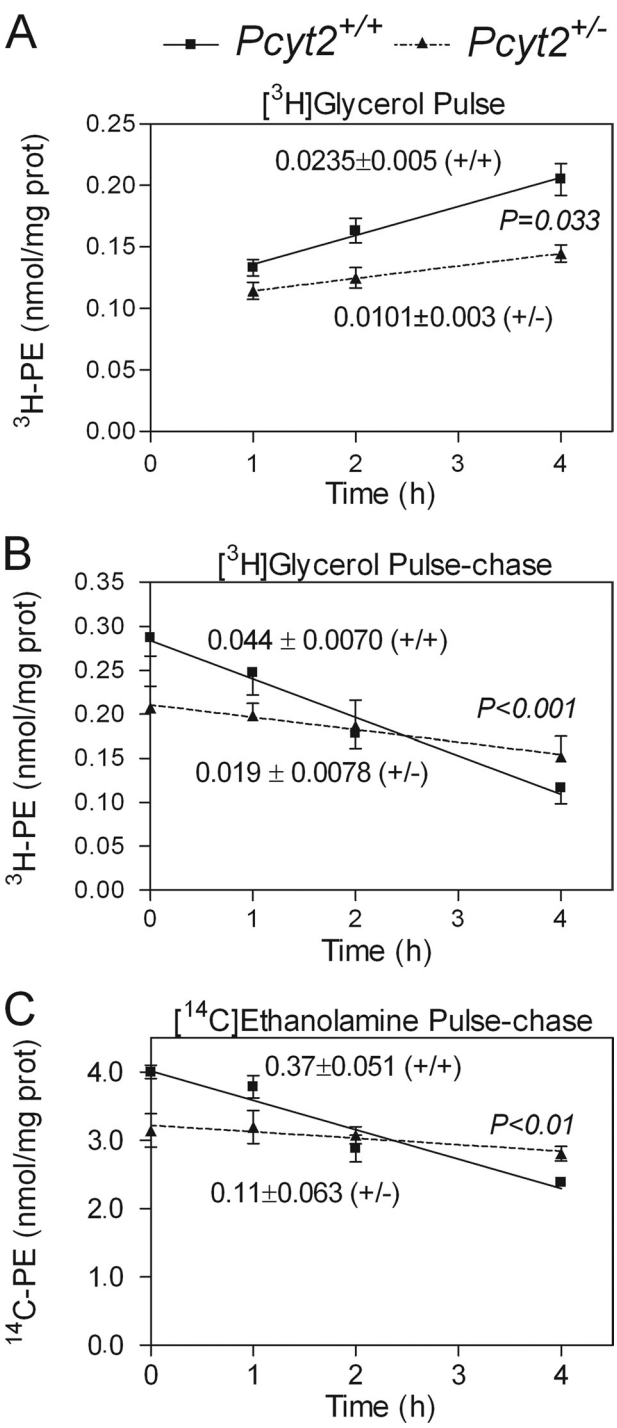

FIGURE 2. **PE metabolism is altered in heterozygous mice.** *A*, rate of PE synthesis from [^{3}H]glycerol pulse experiments in hepatocytes. *B* and *C*, the rate of PE degradation in hepatocytes using [^{14}C]ethanolamine and [^{3}H]glycerol, respectively; studies utilized at least four livers/group from 32–36-week-old mice and were performed in quadruplicate. The rates for each group are shown, where significant differences are between the rates (slope of the lines).

Pcyt2$^{+/-}$ *Mice Have Altered FA Composition*—FA composition was investigated for plasma and liver phospholipids, TG

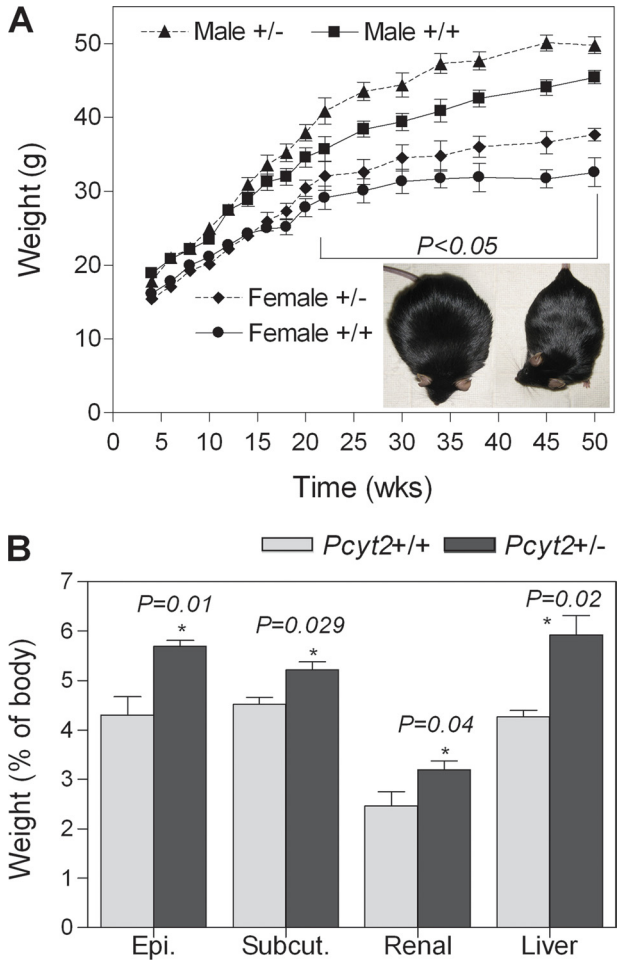

FIGURE 3. ***Pcyt2*$^{+/-}$ mice gain weight chronically.** *A*, increased body weight (from 4 to 50 weeks) for *Pcyt2*$^{+/-}$ and control littermates of both genders (n = at least 16/group); *inset* shows *Pcyt2*$^{+/-}$ and littermate control comparison at ~40 weeks of age. *B*, adipose and liver weights as a percentage of body weight (n = 8/group). *Epi.*, epididymal; *Subcut.*, subcutaneous.

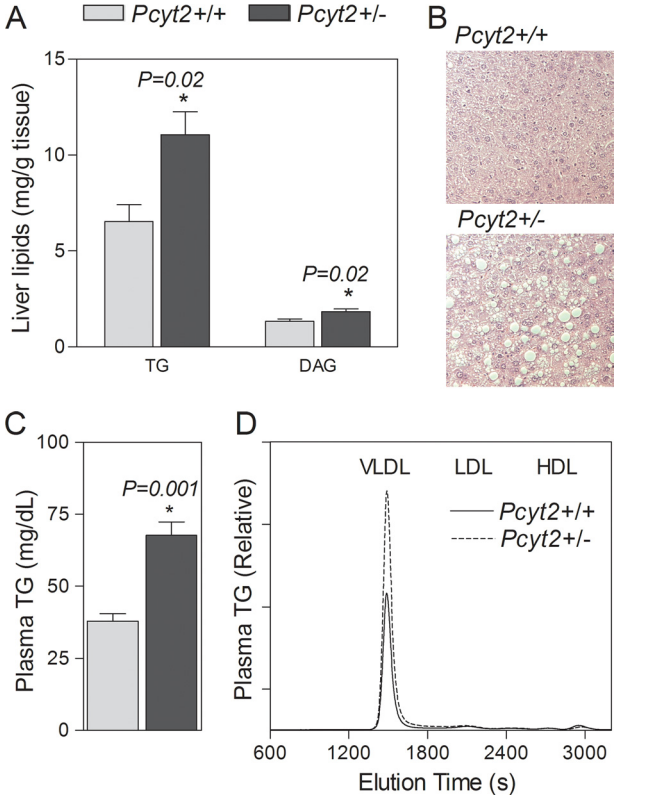

FIGURE 4. ***Pcyt2*$^{+/-}$ mice have fatty liver and hypertriglyceridemia.** *A*, liver TG and DAG content (n = 8/group). *B*, histological analyses of *Pcyt2*$^{+/-}$ and control livers, fixed in paraffin, sectioned at 10 μM, and stained with hematoxylin and eosin (×100); the values are representative of at least four mice for each genotype. *C* and *D*, total plasma TG (n = 8/group, *C*) and lipoprotein profile of plasma TG (n = 6/group, *D*). The results are from 32–36-week-old mice. *VLDL*, very low density lipoprotein; *LDL*, low density lipoprotein; *HDL*, high density lipoprotein.

and DAG. Previously we established that *Pcyt2*$^{+/-}$ mice have significantly reduced polyunsaturated FA content in liver PE (22), mainly contributed from lower arachidonic acid and docosahexaenoic acid. *Pcyt2*$^{+/-}$ liver PS and DAG also had less arachidonic acid, whereas PC FA composition did not significantly differ from control animals (22). *Pcyt2*$^{+/-}$ plasma and liver TG FA composition were also noticeably altered (supplemental Table S1). *Pcyt2*$^{+/-}$ plasma TG had significantly elevated monounsaturated FAs and decreased polyunsaturated FAs, mainly contributed by a dramatic 2-fold elevation in plasma TG oleic acid (C18:1) and reduced C20:3n6 and total omega-6 FA. The FA profile of *Pcyt2*$^{+/-}$ hepatic TG mimicked plasma TG, with elevated C18:1, decreased C18:2n6 and increased total monounsaturated FA content. Increased oleic acid content in *Pcyt2*$^{+/-}$ TG may be indicative of elevated SCD1 (stearoyl-CoA acid desaturase 1) activity, which produces oleic acid as well as an elevated DAG acyltransferase (DGAT) activity, for which oleic acid is a preferred substrate in the final step of TG synthesis (32). Furthermore the FA composition of plasma PC was not altered. Together with the previous findings on modified PE FA composition (22) and the fact that *Pcyt2*$^{+/-}$ mice develop obesity, fatty liver, and hypertriglyceridemia, the FA composition data suggest that in *Pcyt2*$^{+/-}$ mice PE and TG homeostasis are tightly linked, independently of other glycerolipids, most likely via a common intermediate (DAG) (Fig. 1).

Triglyceride Synthesis Is Increased in Pcyt2$^{+/-}$ *Mice*—We next sought to delineate the possible mechanisms for the modified PE, DAG, and TG homeostasis that was facilitating the metabolic phenotype in *Pcyt2*$^{+/-}$ mice. The synthesis (pulse) and degradation (pulse-chase) of TG, DAG, and total phospholipids were evaluated in primary hepatocytes of 32–36-week-old mice using [^{3}H]glycerol radiolabeling. As shown in Fig. 5*A*, total phospholipid synthesis, which mainly reflects the PC synthesis, was not different between genotypes. As described earlier in Fig. 2*A*, the PE synthesis from [^{3}H]glycerol was reduced in *Pcyt2*$^{+/-}$ mice. The rate of synthesis of DAG and TG from [^{3}H]glycerol were, however, higher in *Pcyt2*$^{+/-}$ hepatocytes compared with controls (DAG, 0.098 ± 0.04 *versus* 0.029 ± 0.03 nmol/mg/h; TG, 1.3 ± 0.4 *versus* 0.5 ± 0.1 nmol/mg/h in Fig. 5, *B* and *C*). Moreover, [^{3}H]glycerol radiolabeling of hepatocytes from younger animals revealed a similar pattern, overall demonstrating that the shift toward enhanced formation of DAG and TG is a direct result of *Pcyt2* gene disruption and not a consequence but a cause of the escalating obesity phenotype. Pulse-chase experiments with [^{3}H]glycerol additionally revealed a faster DAG degradation in *Pcyt2*$^{+/-}$ hepatocytes

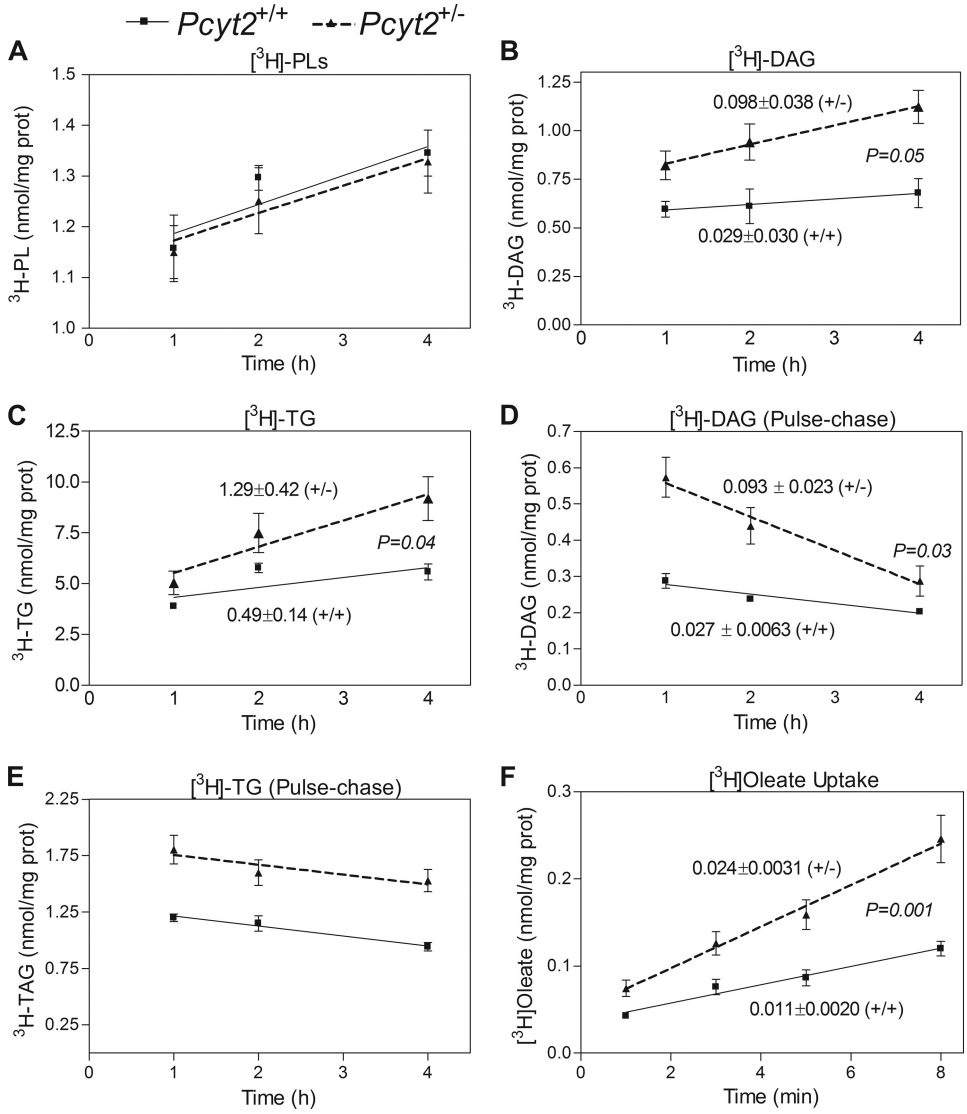

FIGURE 5. ***Pcyt2*$^{+/-}$ mice redirect DAG for TG synthesis and have increased hepatic fatty acid uptake.** *A–C*, pulse experiments with [^{3}H]glycerol demonstrating incorporation into total phospholipids (*PL*), DAG, and TG. *D* and *E*, degradation of DAG and TG assessed by pulse-chase experiments using [^{3}H]glycerol. *F*, hepatic FA uptake ([^{3}H]oleate) (for labeling experiments, at least four livers/group performed in quadruplicate).

(0.09 ± 0.02 *versus* 0.03 ± 0.01 nmol/mg/h) and no changes in TG degradation relative to control hepatocytes (Fig. 5, *D* and *E*). Together these data suggest that the reduced PE synthesis in *Pcyt2*$^{+/-}$ hepatocytes is consistent with the increased rate of DAG production and utilization, which facilitates the redirection of DAG away from PE and toward TG synthesis. Consequently, the accelerated formation of TG rather than its degradation (lipolysis) is responsible for the observed TG accumulation in *Pcyt2*$^{+/-}$ hepatocytes and for the development of liver steatosis (Figs. 3*A* and 4*B*).

Fatty Acid Uptake and de Novo Synthesis Are Elevated in Pcyt2$^{+/-}$ *Mice*—As shown in Fig. 1, additional FAs (acyl-CoA) are required for an elevated TG synthesis from DAG to complete the final step of DAG esterification catalyzed by DGAT. To check whether exogenous FAs are used for DAG and TG synthesis, we performed radiolabeling experiments with [^{3}H]oleate. We established that the rates of DAG and TG synthesis from [^{3}H]oleate were unchanged between genotypes, yet the overall amounts incorporated into DAG and TG were elevated in *Pcyt2*$^{+/-}$ hepatocytes compared with controls (supplemental Fig. S1*A*). This prompted the investigation of FA uptake (Fig. 5*F*), which showed that the [^{3}H]oleate uptake was 2-fold higher in *Pcyt2*$^{+/-}$ hepatocytes compared with littermate controls (23.8 ± 3 *versus* 10.5 ± 2 pmol/mg/min). Interestingly, the content of the FA transport proteins FABPpm, FAT/CD36, FATP1, and FATP4 were unchanged in liver and skeletal muscle (supplemental Fig. S1*B*), demonstrating that their total content is not a reflection of the elevated FA transport efficiency.

The contribution of FA endogenously synthesized from glucose was examined *in vivo* by measuring the incorporation of [^{3}H]acetate into various lipid fractions in both 8- and 36-week-old animals. In both younger and older animals, *Pcyt2*$^{+/-}$ livers had increased [^{3}H]acetate incorporation into DAG and TG and decreased labeling of cholesterol and cholesterol esters. The incorporation of [^{3}H]acetate into free FAs, sphingomyelin, and total phospholipids (PC) did not change and was similar between genotypes (Fig. 6). This demonstrated that in *Pcyt2*$^{+/-}$ mice, the genetic defect in the PE-Kennedy pathway, causes an early increase in *de novo* FA synthesis and adjustments in overall lipid and glucose metabolism prior to the manifestation of symptoms of fatty liver and obesity.

Because acetate (acetyl-CoA) is required for *de novo* synthesis of FA and used in the synthesis of cholesterol (mevalonate pathway), the above data further show that *de novo* FA synthesis (and their incorporation into DAG and TG) in the *Pcyt2*$^{+/-}$ mice were elevated at least in part at the expense of cholesterol biosynthesis/esterification. These data suggest that in addition to reduced PE metabolism, cholesterol metabolism is also reduced in *Pcyt2*$^{+/-}$ mice, which could be required for the proper maintenance of membrane homeostasis in heterozygous animals.

Food Consumption Is Normal in Pcyt2$^{+/-}$ *Mice*—To test whether hyperphagia was contributing to weight gain in *Pcyt2*$^{+/-}$ mice, we monitored food intake for 10 days. At 32 weeks of age, an equal amount of food was consumed between *Pcyt2*$^{+/-}$ and control littermates (3.8 ± 0.8 g/day *versus* 3.9 ± 0.8 g/day). Food intake was also equal in younger animals (8 weeks), indicating no specific role of food consumption in *Pcyt2*$^{+/-}$ obesity.

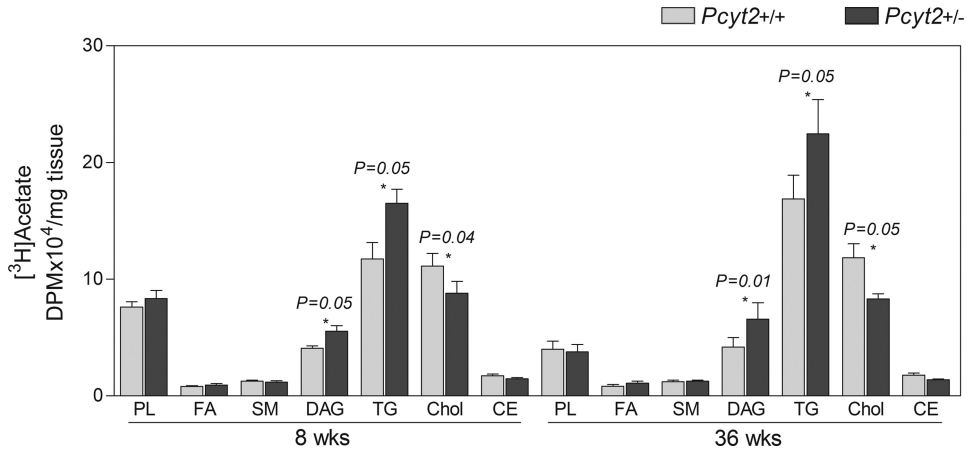

FIGURE 6. **Increased *de novo* lipogenesis in *Pcyt2*$^{+/-}$ livers.** The *in vivo* incorporation of [^{3}H]acetate into hepatic total PL, sphingomyelin (*SM*), FA, DAG, TG, cholesterol (*Chol*), and cholesterol esters (*CE*) for 8- and 36-week-old mice ($n = 6$/group).

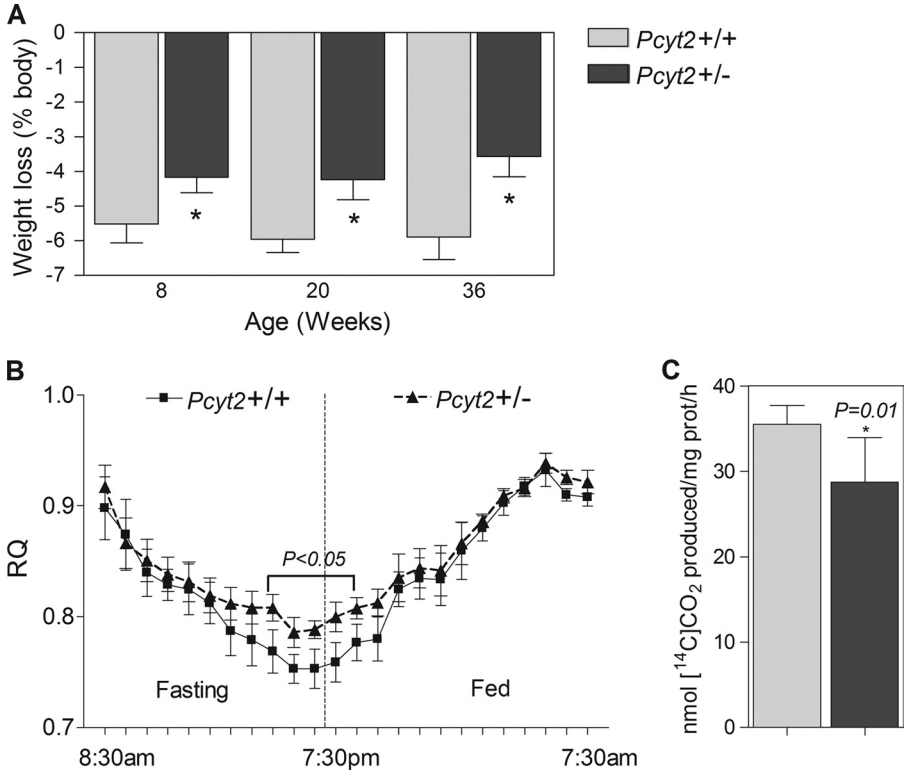

FIGURE 7. **Altered whole body metabolism in *Pcyt2*$^{+/-}$ mice.** *A*, mice (8, 20, and 36 weeks of age) were subjected to a 24-h fast, and weight loss is expressed as a percentage of body weight ($n = 10$/group), where an *asterisk* represents $p < 0.05$, by Student's *t* test. *C*, [^{14}C]oleate oxidation in primary hepatocytes, where the data are expressed as nmol CO_2 produced/mg of protein/h ($n =$ at least three livers analyzed in triplicate). *B*, respiratory quotient (VCO_2/VO_2) determined by indirect calorimetry over a 24-h period; 36-week-old mice were fasted during the light cycle (7:30 am to 7:30 pm) and fed during the dark cycle (7:30 pm to 7:30 am) ($n =$ 5/group). An *asterisk* represents statistical significance ($p < 0.05$) as determined by one-way analysis of variance.

energy expenditure, reflecting a general defect in energy substrate metabolism prior to the development of obesity.

The whole body metabolic measurements using indirect calorimetry displayed an upward shift in the respiratory quotient in *Pcyt2*$^{+/-}$ mice during fasting and during early hours of feeding (Fig. 7*B*), also indicating that the older and already obese *Pcyt2*$^{+/-}$ mice have a decreased capacity for FA utilization as an energy substrate during fasting and an impaired switching to carbohydrate substrate during the fasted-to-fed transition. Finally, when the FA oxidation was measured more directly using [^{14}C]oleate, it was established that oxidation was blunted ~20% in *Pcyt2*$^{+/-}$ primary hepatocytes compared with littermate controls (41.27 ± 1.8 *versus* 52.83 ± 2.7 nmol/mg/h, respectively) (Fig. 7*C*). Therefore, the responses to 24 h of fasting, the upper shift in energy substrate utilization at the whole body level and the reduced FA oxidation in isolated hepatocytes, altogether strongly suggest that *Pcyt2*$^{+/-}$ mice possess an intrinsically reduced capacity for FA utilization in energy production.

Pcyt2$^{+/-}$ *Mice Develop Insulin Resistance*—Because reduced FA oxidation, obesity, and hepatic steatosis have been frequently associated with insulin resistance (33, 34), we further investigated measures of whole body glucose and insulin sensitivity in both young and old *Pcyt2*$^{+/-}$ mice. Fasting levels of *Pcyt2*$^{+/-}$ plasma insulin, glucose, and free FAs were not significantly different from controls; however, when challenged with an intraperitoneal glucose load, both glucose (Fig. 8*A*) and insulin (Fig. 8*B*) were elevated (cleared more slowly from plasma) in 32–36-week-old *Pcyt2*$^{+/-}$ mice relative to controls post-injection, and the areas under the curve in both measurements were significantly increased compared with controls. As in the liver, skeletal muscle DAG and TG content were also significantly increased in older *Pcyt2*$^{+/-}$ mice (Fig. 8*C*). Importantly, 8-week-old *Pcyt2*$^{+/-}$ mice remain insulin-sensitive, demonstrating that the impaired insulin

Energy Expenditure and FA Oxidation Are Diminished in Pcyt2$^{+/-}$ *Mice*—As an initial investigation into the energy requirements of the *Pcyt2*$^{+/-}$ mice, we initiated a 24-h fast in both younger and older animals, after which animals were weighed, and weight loss was recorded. *Pcyt2*$^{+/-}$ animals displayed resistance to weight loss compared with control animals at all of the ages examined (30% at 8 and 20 weeks of age and 35% at 36 weeks of age; Fig. 7*A*), which is indicative of a lower

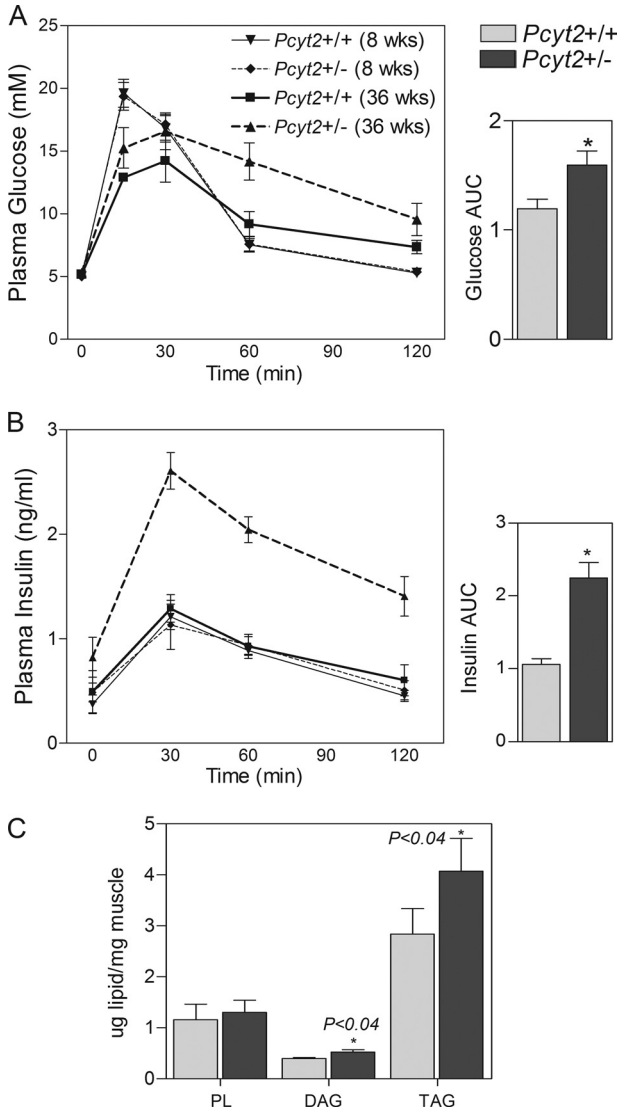

FIGURE 8. **Reduced insulin sensitivity and increased muscle lipid accumulation in *Pcyt2*$^{+/-}$ mice.** *A*, intraperitoneal glucose tolerance test (IPGTT); where glucose levels were from base line to 120 min ($n = 6$/group). *B*, IPGTT insulin levels from base line to 120 min ($n = 6$/group). Area under the curve for IPGTT glucose and area under the curve for IPGTT insulin are for 36-week old mice. For *C* and *D*, an *asterisk* represents statistical significance ($p < 0.05$). *E*, total PL, DAG, and TG content of skeletal muscle of 36-week-old mice ($n = 8$).

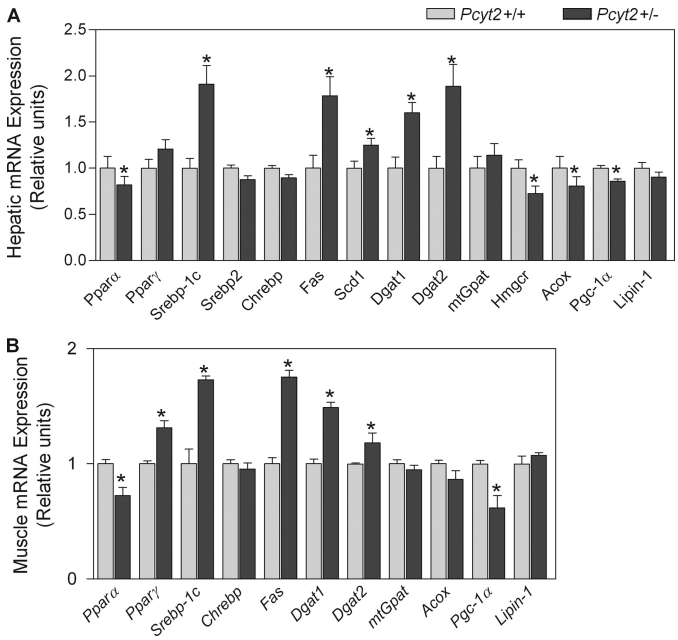

FIGURE 9. **Altered *Pcyt2*$^{+/-}$ hepatic and skeletal muscle mitochondrial and lipogenic gene expression.** *A* and *B*, hepatic and skeletal muscle mRNA expression, relative to β-actin as an endogenous control and relative to littermate controls, set to 1 ($n = 8$/group, 36-week-old mice). The analyses were performed in triplicate. *Ppar*, peroxisome proliferator-activated receptor; *Srebp*, sterol regulatory element-binding protein; *Chrebp*, carbohydrate response element-binding protein; *Fas*, fatty acid synthase; *Scd1*, stearoyl-CoA desaturase-1; *Dgat*, diacylglycerol acyltransferase; *mtGpat*, mitochondrial glycerol 3-phosphate acyltransferase; *Hmgcr*, 3-hydroxy-3-methylglutaryl-CoA reductase; *Acox1*, acyl-CoA oxidase-1; *Pgc-1α*, peroxisome proliferator-activated receptor co-activator 1α. An *asterisk* represents statistical significance ($p < 0.05$).

sensitivity and glucose metabolism are consequences not causes of *Pcyt2*$^{+/-}$ metabolic phenotype.

Expression Pattern of Lipogenic Genes Is Modified in Pcyt2$^{+/-}$ *Liver and Muscle*—The gene expression patterns of the 36-week-old *Pcyt2*$^{+/-}$ muscle and liver for several lipogenic transcription factors and their corresponding downstream targets indicated an altered transcription of key lipid enzymes and regulators (Fig. 9). The insulin- and glucose-responsive *Srebp1*, a key regulator of lipogenesis, was up-regulated in both *Pcyt2*$^{+/-}$ liver and muscle. The increased expression of *Srebp1* may in turn be responsible for the increased transcription of *Fas* and *Scd1* in both tissues and is in keeping with the [^{3}H]acetate radiolabeling and FA composition data, showing an elevated FA *de novo* synthesis and an increased oleate content in *Pcyt2*$^{+/-}$ TG. *Pcyt2*$^{+/-}$ liver and muscle also had enhanced expression of both *Dgat1* and *Dgat2*, which could explain the observed accumulation of TG in both liver and muscle and is in agreement with the [^{3}H]glycerol data showing an elevated TG synthesis. The mitochondrial glycerol-3-phosphate acyltransferase and lipin-1 (phosphatidic acid phosphatase), the subsequent enzymes involved in the formation of lysophosphatidic acid and DAG from glycerol-3 phosphate considered as the main regulators of TG synthesis, were not altered, suggesting that the DAG esterification step catalyzed by DGAT was more critical to drive the TG synthesis in *Pcyt2*$^{+/-}$ mice. In keeping with the evidence that heterozygous animals have an impaired ability to oxidize FA, markers of mitochondrial biogenesis as well as oxidation were significantly reduced in *Pcyt2*$^{+/-}$ liver and muscle, such as liver peroxisome proliferator-activated receptor α, peroxisome proliferator activated receptor co-activator 1α, and liver acyl-CoA oxidase. Also, *Pcyt2*$^{+/-}$ livers had moderately reduced expression of 3-hydroxy-3-methylglutaryl-CoA reductase, the rate-limiting enzyme in cholesterol biosynthesis, in agreement with the moderately reduced incorporation of [^{3}H]acetate into cholesterol. Therefore, these alterations in gene expression in *Pcyt2*-deficient animals support the observed metabolic phenotype, where genetically reduced PE synthesis caused a shift in the balance between membrane lipids, energy storage, and production and gradually progressed to the metabolic syndrome phenotype at older age.

DISCUSSION

In the past, there have been select lines of evidence that have highlighted the relationship between phospholipids (mainly PC), DAG, and TG metabolism (35–37). DAG and FA released from phospholipids can be utilized for TG synthesis (38), and alterations in cellular PC content are sufficient to cause changes in TG metabolism (35). In rat hepatocytes, an elevated TG synthesis occurred as a result of excess DAG when CDP-choline was limiting PC synthesis and also where DGAT activity was maximal (39). It has also been established that mutations inhibiting CTP:phosphocholine cytidylyltransferase of the PC-Kennedy pathway in Chinese hamster ovary cells result in a redirection of DAG from phospholipids to TG (35). Interestingly, in *Drosophila*, inhibition of PC synthesis increased TG content in lipid droplets, mainly by altering the size and the morphology of the droplets (40). In a mammalian context, a liver-specific CTP:phosphocholine cytidylyltransferase α knock-out model was shown to have decreased very low density lipoprotein secretion and therefore accumulated TG in the liver because of reduced PC synthesis (41).

The specific interaction between PE and TG metabolism has been largely unexplored. Here we describe for the first time an animal model with genetically reduced PE synthesis, which similarly to the inhibition of PC synthesis via the Kennedy pathway in Chinese hamster ovary cells leads to elevated DAG and TG (35). Surprisingly, however, this also leads to the development of a metabolic disease phenotype. Our results demonstrate a causal effect of *Pcyt2* disruption on the redirection of DAG toward TG formation. The decreased rate of CDP-ethanolamine formation in *Pcyt2*$^{+/-}$ mice reduces the rate of PE synthesis. As a direct consequence, DAG is made available for TG formation, which is further facilitated by the increased formation/availability of FA.

It is common for the up-regulation of certain genes in DAG and TG synthesis to result in symptoms of obesity (42–44); however, most genetic knock-out models result in the amelioration of obesity, hepatic steatosis, and insulin resistance (45–47). Before this study, it was not known that obesity and insulin resistance could manifest because of irregularities in membrane phospholipid homeostasis. *Pcyt2*$^{+/-}$ mice are indistinguishable from littermate controls during the first stages of postnatal development and remain so until ~24 weeks of age. Young (8–20 weeks) mice, however, experience a metabolic phenotype similar to the older (obese) animals that is characterized by a chronic state of decreased FA oxidation and increased FA synthesis, resulting in an increase in TG formation. This represents an inherent shift in glycerolipid metabolism together with an increased partitioning of FA toward storage (away from oxidation), causing a more positive energy balance and being most likely responsible for the chronic disease progression. There appears to be a threshold (~24–28 weeks) after which the heterozygous animals become significantly heavier than control animals and experience hypertriglyceridemia, hepatic TG accumulation, and insulin resistance.

Various lipid intermediates such as DAG, ceramide, and free FAs negatively regulate the insulin signaling cascade and are frequently elevated in obesity and insulin resistance (41, 48). We believe that increased DAG availability caused by reduced production of CDP-ethanolamine may play a major role in the development of obesity and insulin resistance in *Pcyt2*-deficient mice, although the role of ceramides in the progression of this phenotype cannot be ruled out in the current investigation. Although young *Pcyt2*$^{+/-}$ animals possess a metabolic defect similar to the older animals (reduced PE synthesis, increased lipogenesis/TG formation, and decreased FA oxidation), they are neither obese nor have they lost their sensitivity to insulin. It would then seem logical that the alterations in lipid metabolism are adaptive measures to prevent the accumulation of toxic amounts of DAG, unused in PE synthesis. Because additional FAs are needed for DAG esterification, the metabolic labeling and gene expression studies showed that they were made available by several processes including an elevated *de novo* FA synthesis and reduced acetyl-CoA participation in cholesterol synthesis/esterification and by reduction in FA oxidation (an increased utilization of glucose as a source of energy and acetyl-CoA production). The mechanisms that interfere with the ability of insulin to regulate glucose metabolism in *Pcyt2*-deficient mice required further analyses, and investigations are currently under way.

Studies have shown an inverse relationship between intramyocellular TG storage and insulin sensitivity in both rodent and human models (49); however, trained athletes have the highest levels of both intramuscular TG and insulin sensitivity (50). There is increasing evidence that supports a role for increased levels of active lipid intermediates rather than TG itself, which may play more critical roles in the impairment of insulin signaling (48, 51). Overexpression of *Dgat1* in mouse skeletal muscle (resulting in a 3-fold increase in acyltransferase activity) increased TG formation, yet improved insulin sensitivity by decreasing levels of DAG (52). Although we believe that young *Pcyt2*$^{+/-}$ animals potentially use similar means to eliminate excess DAG, our model suggests the possibility that a threshold may exist, where at a certain point the elimination of DAG via endogenous TG synthesis (DGAT pathway) may no longer be capable of acting as a protective mechanism. Particularly, this could be the case developmentally. We have shown that younger *Pcyt2*$^{+/-}$ mice experience elevated lipogenesis; however, they develop fatty liver, obesity, and insulin resistance at later stages. The important consequence of chronically elevated lipogenesis in *Pcyt2*$^{+/-}$ mice is an increased DAG accumulation, which may eventually become lipotoxic in older animals. This accumulation would most likely act by modulating the activities of DAG-dependent novel protein kinase C isoforms (53, 54), the well established players in insulin resistance (55). We show that key metabolic genes become altered in the liver and skeletal muscle of old *Pcyt2*$^{+/-}$ mice. However, it remains to be determined when exactly during development the expressions of these specific genes become critically impaired, as well as which key metabolic and regulatory pathways are the main triggers of the *Pcyt2*$^{+/-}$ phenotype.

The disruption of *Pcyt2* is not only responsible for alteration in DAG and TG synthesis but also affects other aspects of cellular lipid metabolism, such as reduced cholesterol synthesis and FA oxidation. *Pcyt2* heterozygous animals possess an inherent defect in energy metabolism, which could be an over-

compensation in response to the altered DAG levels but could also be a result of impaired lipolysis and reduced PE availability as a source of FA, which is an interesting area for further investigation. Considerable efforts have been made to understand phospholipid catabolism, and multiple lipases/phospholipases have been established as significant contributors to the above pathologies. However, it is equally important to understand the anabolic aspects of phospholipid metabolism, including *de novo* PE biosynthesis. The *Pcyt2*-deficient model is unique and offers a new description for the development of obesity-related disorders. It will increase our understanding of the PE-Kennedy pathway at the whole body level and further affirm the importance of the *Pcyt2* gene in lipid metabolism.

Acknowledgments—We thank Laelie Snook for conducting experiments on fatty acid transport protein expression and Jamie Lally for help with real time PCR. We thank the group in the Molecular and Cell Biology of Lipids (University of Alberta) for lipoprotein analyses. We thank Vera Michel, Angela Tie, and Jessica Fullerton for reading this manuscript and for helpful discussions.

REFERENCES

1. Bakovic, M., Fullerton, M. D., and Michel, V. (2007) *Biochem. Cell Biol.* **85,** 283–300
2. McFarland, M. J., and Barker, E. L. (2004) *Pharmacol. Ther.* **104,** 117–135
3. Menon, A. K., and Stevens, V. L. (1992) *J. Biol. Chem.* **267,** 15277–15280
4. Steenbergen, R., Nanowski, T. S., Beigneux, A., Kulinski, A., Young, S. G., and Vance, J. E. (2005) *J. Biol. Chem.* **280,** 40032–40040
5. Ortlund, E. A., Lee, Y., Solomon, I. H., Hager, J. M., Safi, R., Choi, Y., Guan, Z., Tripathy, A., Raetz, C. R., McDonnell, D. P., Moore, D. D., and Redinbo, M. R. (2005) *Nat Struct. Mol. Biol.* **12,** 357–363
6. Dobrosotskaya, I. Y., Seegmiller, A. C., Brown, M. S., Goldstein, J. L., and Rawson, R. B. (2002) *Science* **296,** 879–883
7. Arthur, G., and Page, L. (1991) *Biochem. J.* **273,** 121–125
8. Bleijerveld, O. B., Brouwers, J. F., Vaandrager, A. B., Helms, J. B., and Houweling, M. (2007) *J. Biol. Chem.* **282,** 28362–28372
9. Borkenhagen, L. F., Kennedy, E. P., and Fielding, L. (1961) *J. Biol. Chem.* **236,** 28–30
10. Voelker, D. R., and Frazier, J. L. (1986) *J. Biol. Chem.* **261,** 1002–1008
11. Sundler, R., Akesson, B., and Nilsson, A. (1974) *FEBS Lett.* **43,** 303–307
12. Min-Seok, R., Kawamata, Y., Nakamura, H., Ohta, A., and Takagi, M. (1996) *J Biochem.* **120,** 1040–1047
13. Nakashima, A., Hosaka, K., and Nikawa, J. (1997) *J. Biol. Chem.* **272,** 9567–9572
14. Bladergroen, B. A., Houweling, M., Geelen, M. J., and van Golde, L. M. (1999) *Biochem. J.* **343,** 107–114
15. Poloumienko, A., Coté, A., Quee, A. T., Zhu, L., and Bakovic, M. (2004) *Gene* **325,** 145–155
16. Tie, A., and Bakovic, M. (2007) *J. Lipid Res.* **48,** 2172–2181
17. Johnson, C. M., Yuan, Z., and Bakovic, M. (2005) *Biochim. Biophys. Acta* **1735,** 230–235
18. Zhu, L., Johnson, C., and Bakovic, M. (2008) *J. Lipid Res.* **49,** 2197–2211
19. Tijburg, L. B., Houweling, M., Geelen, M. J., and Van Golde, L. M. (1989) *Biochem. J.* **257,** 645–650
20. Jamil, H., Utal, A. K., and Vance, D. E. (1992) *J. Biol. Chem.* **267,** 1752–1760
21. Houweling, M., Tijburg, L. B., Vaartjes, W. J., and van Golde, L. M. (1992) *Biochem. J.* **283,** 55–61
22. Fullerton, M. D., Hakimuddin, F., and Bakovic, M. (2007) *Mol. Cell. Biol.* **27,** 3327–3336
23. Bligh, E. G., and Dyer, W. J. (1959) *Can. J. Biochem. Physiol.* **37,** 911–917
24. Igal, R. A., Pallanza de Stringa, M. C., and Tacconi de Gómez Dumm, I. N. (1994) *Int. J. Biochromatogr.* **1,** 137–142
25. Denomme, J., Stark, K. D., and Holub, B. J. (2005) *J. Nutr.* **135,** 206–211
26. Klaunig, J. E., Goldblatt, P. J., Hinton, D. E., Lipsky, M. M., Chacko, J., and Trump, B. F. (1981) *In Vitro* **17,** 913–925
27. Klaunig, J. E., Goldblatt, P. J., Hinton, D. E., Lipsky, M. M., and Trump, B. F. (1981) *In Vitro* **17,** 926–934
28. Bonen, A., Han, X. X., Habets, D. D., Febbraio, M., Glatz, J. F., and Luiken, J. J. (2007) *Am. J. Physiol. Endocrinol. Metab.* **292,** E1740–E1749
29. Lewin, T. M., Wang, S., Nagle, C. A., Van Horn, C. G., and Coleman, R. A. (2005) *Am. J. Physiol. Endocrinol. Metab.* **288,** E835–E844
30. Steenbergen, R., Nanowski, T. S., Nelson, R., Young, S. G., and Vance, J. E. (2006) *Biochim. Biophys. Acta* **1761,** 313–323
31. Wu, G., Aoyama, C., Young, S. G., and Vance, D. E. (2008) *J. Biol. Chem.* **283,** 1456–1462
32. Ntambi, J. M., and Miyazaki, M. (2004) *Prog. Lipid Res.* **43,** 91–104
33. Jiang, J., and Torol, N. (2008) *Metab. Syndr. Relat. Disord.* **6,** 1–7
34. Petersen, K. F., and Shulman, G. I. (2006) *Am. J. Med.* **119,** (Suppl. 1) S10–S16
35. Caviglia, J. M., De Gómez Dumm, I. N., Coleman, R. A., and Igal, R. A. (2004) *J. Lipid Res.* **45,** 1500–1509
36. Igal, R. A., and Coleman, R. A. (1998) *J. Lipid Res.* **39,** 31–43
37. Vance, D. E. (2008) *Curr. Opin. Lipidol.* **19,** 229–234
38. Igal, R. A., Caviglia, J. M., de Gómez Dumm, I. N., and Coleman, R. A. (2001) *J. Lipid Res.* **42,** 88–95
39. Stals, H. K., Top, W., and Declercq, P. E. (1994) *FEBS Lett.* **343,** 99–102
40. Guo, Y., Walther, T. C., Rao, M., Stuurman, N., Goshima, G., Terayama, K., Wong, J. S., Vale, R. D., Walter, P., and Farese, R. V. (2008) *Nature* **453,** 657–661
41. Jacobs, R. L., Devlin, C., Tabas, I., and Vance, D. E. (2004) *J. Biol. Chem.* **279,** 47402–47410
42. Lindén, D., William-Olsson, L., Ahnmark, A., Ekroos, K., Hallberg, C., Sjögren, H. P., Becker, B., Svensson, L., Clapham, J. C., Oscarsson, J., and Schreyer, S. (2006) *FASEB J.* **20,** 434–443
43. Millar, J. S., Stone, S. J., Tietge, U. J., Tow, B., Billheimer, J. T., Wong, J. S., Hamilton, R. L., Farese, R. V., Jr., and Rader, D. J. (2006) *J. Lipid. Res.* **47,** 2297–2305
44. Nagle, C. A., An, J., Shiota, M., Torres, T. P., Cline, G. W., Liu, Z. X., Wang, S., Catlin, R. L., Shulman, G. I., Newgard, C. B., and Coleman, R. A. (2007) *J. Biol. Chem.* **282,** 14807–14815
45. Abu-Elheiga, L., Oh, W., Kordari, P., and Wakil, S. J. (2003) *Proc. Natl. Acad. Sci. U.S.A.* **100,** 10207–10212
46. Hammond, L. E., Gallagher, P. A., Wang, S., Hiller, S., Kluckman, K. D., Posey-Marcos, E. L., Maeda, N., and Coleman, R. A. (2002) *Mol. Cell. Biol.* **22,** 8204–8214
47. Smith, S. J., Cases, S., Jensen, D. R., Chen, H. C., Sande, E., Tow, B., Sanan, D. A., Raber, J., Eckel, R. H., and Farese, R. V., Jr. (2000) *Nat. Genet.* **25,** 87–90
48. Timmers, S., Schrauwen, P., and de Vogel, J. (2008) *Physiol. Behav.* **94,** 242–251
49. Phillips, D. I., Caddy, S., Ilic, V., Fielding, B. A., Frayn, K. N., Borthwick, A. C., and Taylor, R. (1996) *Metabolism* **45,** 947–950
50. Goodpaster, B. H., He, J., Watkins, S., and Kelley, D. E. (2001) *J. Clin. Endocrinol. Metab.* **86,** 5755–5761
51. Summers, S. A. (2006) *Prog. Lipid Res.* **45,** 42–72
52. Liu, L., Zhang, Y., Chen, N., Shi, X., Tsang, B., and Yu, Y. H. (2007) *J. Clin. Invest.* **117,** 1679–1689
53. Yu, C., Chen, Y., Cline, G. W., Zhang, D., Zong, H., Wang, Y., Bergeron, R., Kim, J. K., Cushman, S. W., Cooney, G. J., Atcheson, B., White, M. F., Kraegen, E. W., and Shulman, G. I. (2002) *J. Biol. Chem.* **277,** 50230–50236
54. Griffin, M. E., Marcucci, M. J., Cline, G. W., Bell, K., Barucci, N., Lee, D., Goodyear, L. J., Kraegen, E. W., White, M. F., and Shulman, G. I. (1999) *Diabetes* **48,** 1270–1274
55. Schmitz-Peiffer, C. (2002) *Ann. N. Y. Acad. Sci.* **967,** 146–157